

Large scale model test for the determination of the structural behavior of a geogrid-reinforced slope

H. Zanzinger & E. Gartung
LGA-Institute of Foundation Engineering, Nuremberg, Germany

ABSTRACT: A model test was executed on a sand-geogrid-wall with a face inclined at 85° , height 3.70 m, length 2.80 m, depth of the model 4.30 m. The well compacted sand was reinforced by 7 layers of PVC-coated PET-grid-fabric. The retaining structure was loaded to failure under earth pressure induced by a strip footing. The extensive internal and external instrumentation gave a complete record of the deformation and load bearing behavior of the model throughout the test. It was found, that the failure can be described very accurately by a sliding mechanism of two kinematic elements. So the computational method developed for the stability analysis has been verified by the large scale physical model test.

1 STABILITY ANALYSIS OF MULTILAYERED GEOTEXTILE REINFORCED SOIL RETAINING STRUCTURES

The structural analysis of steep slopes reinforced by geotextiles considers sliding failure of the reinforced soil body on plane or curved sliding surfaces below the retaining structure, base failure and overturning as possible failure modes, against which a sufficient safety margin has to be warranted. Limit equilibrium analyses with the assumption that the reinforced soil body behaves as a rigid block are the appropriate and well established methods for the determination of the external stability. The modes of internal failure of reinforced soil structures are accounting for breakage of the reinforcing elements, pullout of the reinforcement, local failure of the face of the retaining wall and shear failure of the soil.

Whereas the determination of the stability against external failure modes of geotextile-reinforced bodies is the same as for any other foundation engineering structure, the internal failure modes are governed by the interaction of the soil and the inclusions. Due to the complicated nature of this problem, it is not possible to determine the stability of multilayered soil-geotextile structures on a purely theoretical basis (Schlosser 1990). It is necessary to study the soil-inclusion interaction by experiments of adequate size. So, for the introduction of a new woven polyester-geogrid, large scale model tests were carried out to understand the performance of a steep slope reinforced soil retaining wall under lateral earth pressures, and to verify the proposed analytical model (Zanzinger, Gartung 1992). The analysis of internal stability is based on the kinematic element method. The limit equilibrium of two rigid blocks with variable geometry is determined for the condition that the ratio of the resisting forces ($\sum Z_i$) to the translational driving forces of the kinematic system reaches a minimum (fig. 1).

A computer program was developed for the analysis and applied to the prediction of the failure load of the large

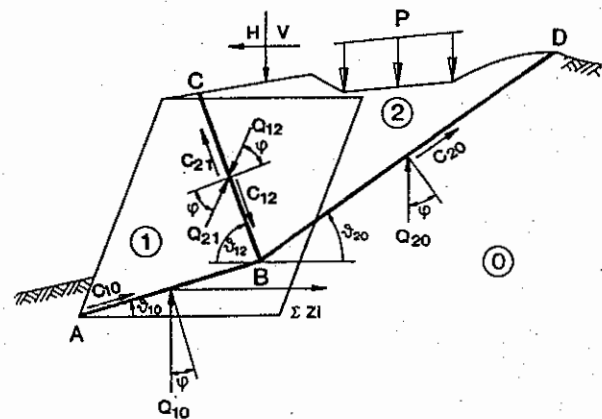


Fig.1 Two blocks sliding failure mechanism

scale model test (Pressl, Zanzinger 1991). For the boundary conditions and material properties described in the following paragraphs, a factor of safety against internal failure of $\eta = 1,0$ was obtained at an earth pressure induced by a vertical surcharge load of $F = 1350$ kN.

2 BOUNDARY CONDITIONS OF THE MODEL TEST

The multilayered reinforced soil retaining structure was composed of sand and geogrids. Above a 50 cm base layer of compacted sand at the bottom, seven composite layers of 51 cm each were placed in the test pit, so the total height of the model amounted to about 4.10 m. The spacing of the geogrids coincided with openings of the bulkhead at the backface of the model, through which extensometer wires could be carried (fig. 2), furthermore this spacing represents field conditions reasonably well. The width of the model was 2.75 m matching the length of the concrete beam which was

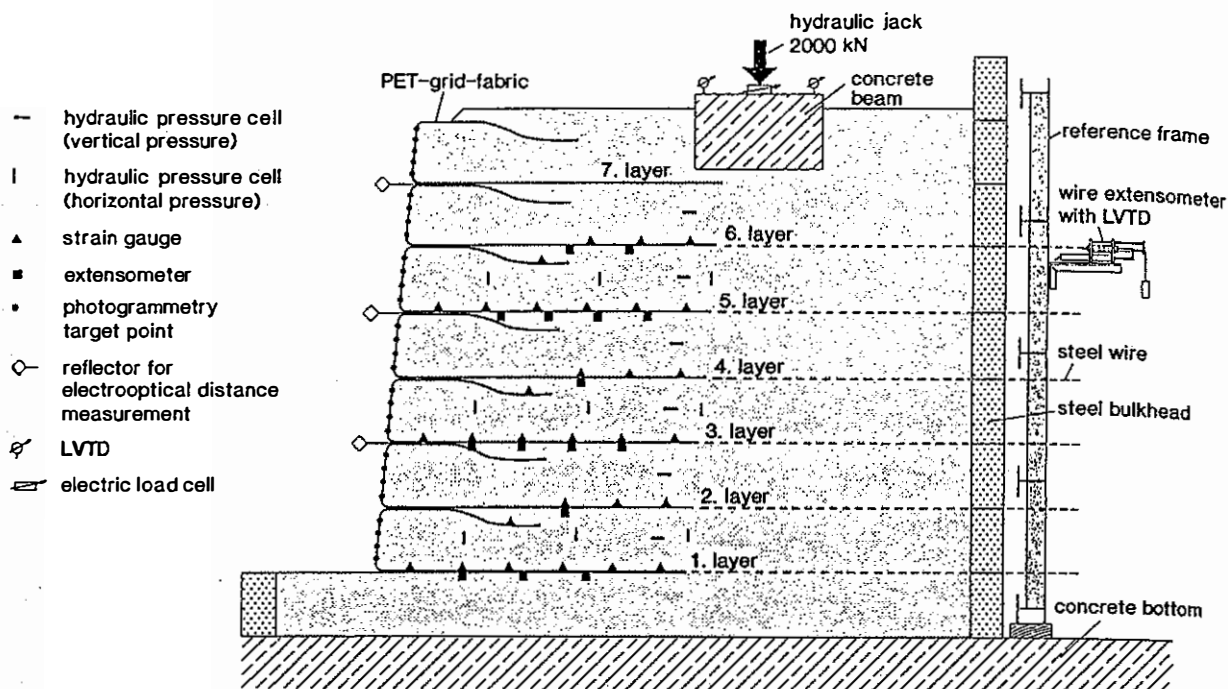


Fig.2 Cross section and instrumentation

used for load application (2.70 m x 1.00 m x 0.60 m). Since German design rules for reinforced earth structures recommend a length of the reinforcing elements of $0.7 \cdot H$, where H is the height of the structure, the embedded length of the geogrid was chosen as 2.5 m at the bottom of each sand layer, and it was 1.3 m at the top to secure sufficient anchorage for the support of the local earth pressure acting at the face (Bundesminister für Verkehr 1985).

The model set up was such that the lateral earth pressure induced by a vertical load applied through hydraulic jack upon the concrete beam could act upon the multilayered reinforced soil retaining structure and load it until failure. The embedment of the concrete beam was sufficient to prevent local base failure. At the backface and at the side walls of the soil body, two sheets of nonwoven geotextiles with a smooth geomembrane sandwiched in between were installed for the reduction of wall friction. The influence of the remaining frictional resistance at the walls was quantitatively taken into account. The friction angle of the sandwiched geosynthetics was determined at about 11° by direct shear tests on samples of the geosynthetics (300 mm x 300 mm).

3 PROPERTIES OF THE TEST SOIL

The test soil consisted of a very uniform medium sand. It was placed in a dry condition (at a water content of 1.8 %), and compacted to a relative density of 84 %. The plane strain peak angle of friction was determined at $\phi' = 41^\circ$ by direct shear tests in a shear box 300 mm x 300 mm. The relevant properties of the soil are summarised on table 1, the gradation curve is presented on fig. 3.

Table 1. Properties of test soil

Coefficient of uniformity	U	3
Water content	w	1.78 %
Max. dry density	γ_{dmax}	1.83 t/m ³
Min. dry density	γ_{dmin}	1.47 t/m ³
Min. void ratio	e_{min}	0.45
Max. void ratio	e_{max}	0.80
Placement bulk density	γ_{pl}	1.79 t/m ³
Placement dry density	γ_{dpl}	1.76 t/m ³
Placement void ratio	e	0.51
Placement relative density	I_D	84 %
Placement friction angle	ϕ'_{pl}	41 °

4 PROPERTIES OF THE GEOGRID

The geogrid consists of a woven polyester-yarn fabric (PET) coated by polyvinylchloride (PVC). The PVC-coating protects the high-strength PET-fibers against chemical, biological and other environmental influences, it fixes the knots where warp and weft yarns are crossing, and it facilitates handling and installation of the geogrid without mechanical damage to the sensitive PET-fibers. The wide meshed geogrid shows good shear-bond properties in soils. By direct shear tests (300 mm x 300 mm samples) the apparent angle of frictional resistance between the geogrid and the test-soil was determined at 41° which amounts to 100 % of the peak friction angle of the test soil.

The tensile strength of the geogrid is 64.7 kN/m in warp and 32.4 kN/m in weft direction at failure strains of 12.9 % and 12.2 % respectively. The influence of creep is negligible

Table 2. Properties of the geogrid

Mass per unit area	471 g/m ²	
Thickness	warp strands	1.92 mm
	weft strands	1.83 mm
	knot	1.90 mm
Spacing of	warp strands	15.9 mm
	weft strands	18.2 mm
Width of PVC-coated	warp strands	3.3 mm
	weft strands	2.6 mm
Tensile strength	warp direction	64.7 kN/m
	weft direction	32.4 kN/m
Strain at peak tensile stress	warp direction	12.9 %
	weft direction	12.2 %
Secant modulus at 5 % strain	warp direction	404 kN/m
	weft direction	218 kN/m
Creep strain under 25 % of short term tensile strength after 21 days	warp direction	1.44 %
	weft direction	1.46 %
Knot strength	warp direction	246 N
	weft direction	286 N
Frictional resistance in contact with medium dense sand	$K\phi$ ¹⁾	1.0

$$1) K\phi = \frac{\tan \phi_{\text{contact}}}{\tan \phi_{\text{sand}}}$$

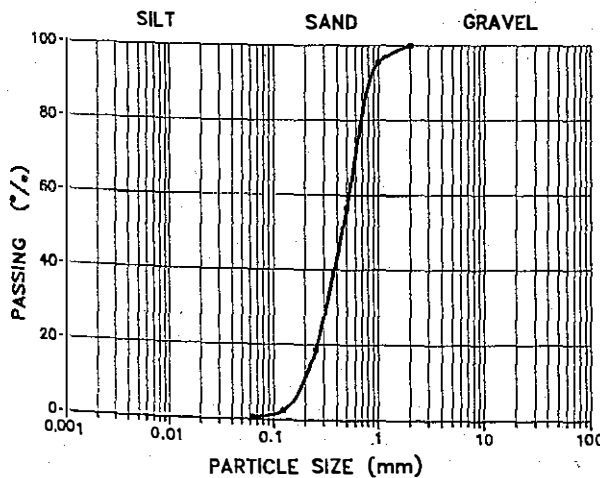


Fig.3 Particle size distribution curve of the test sand

under service-loads. Table 2 lists the relevant material properties of the geogrid which were determined at the laboratory of LGA-Institute of Foundation Engineering, Nuremberg.

5 INSTRUMENTATION

The performance of the model was monitored by a measurement system which gave information about the visible deformations of the reinforced soil block and about the internal response to loading. Since the load application was the governing parameter of the test, much attention had to be paid to the measurement of the applied force by means of an electrical transducer whose signals were fed into the computer for recording and test control. The settlement of the concrete beam was measured at the four corners by electrical displacement transducers LVTDs. In combination with electrooptical distance measurements of three spots at the face of the retaining wall and surface levelling, these data gave an immediate information about the behavior of the model during the test. A complete three dimensional image of the surface displacements was obtained by photogrammetric surveying. More than 200 target points were spread across the model along seven vertical sectionlines and 25 targets at the boundaries. Photographic recording of these targets from various positions at different stages of the test and processing by digital scanner and computer gave precise and encompassing information about the surface displacements.

The internal instrumentation consisted of 15 extensometers, 30 strain gauges and 15 hydraulic pressure cells. The instruments were placed in a pattern that matches the multi-layered structural system. Fig. 2 also indicates how the displacement measurements of the wire extensometers were transmitted to LVTDs behind the reference frame. The measuring points of the extensometers consisted of small brass platens attached to knots of the geogrid. To avoid any considerable passive resistance, they were covered by rubber sleeves. The 1 mm thick high strength steel wires of the extensometers were protected by plastic tubes which permitted free movement of the wires.

The strain gauges were attached to the PVC-surface of the geogrid. Previous investigations had shown that the strain of the PET-strings could be measured correctly in this way. So the tensile forces within the geogrid layers could be deduced directly from the strain gauge measurements which were fed into the computer like all other electrical signals.

The readings of the hydraulic pressure cells were recorded manually. The pressure cells of the type Glözl E20/30 were arranged in three vertical sections for the measurement of horizontal stresses and in one line for the measurement of vertical stresses at six elevations.

6 INSTALLATION OF THE MULTILAYERED MODEL

After placement and compaction of the bottom layer of sand of 50 cm thickness, the first geogrid with strain gauges and extensometers attached to it was installed. Sand filled jute-sacks were used to form the face of the retaining structure. The sand layer of 51 cm thickness was placed in two lifts

and compacted by a vibrating steel plate (1.44 m², 2.5 kN, 1800 - 2000 rpm). The anchoring part of the geogrid of 1.3 m length was carefully wrapped around the jute sacks, positioned and covered by sand. This procedure of installation was repeated six times. From precise surveying at all stages of construction and weight control of the sand entered into the model, it was determined that a very uniform distribution of the density could be achieved. All operations including the installation of the pressure cells within the body of sand, the layout of connecting tubes and wires, positioning of geogrids, sand sacks and placement and compaction of sand had to be executed with greatest care to avoid disturbances of the soil and to warrant proper functioning of the entire measuring system. It took three weeks to set up the model structure. The working team consisted of one engineer and three skilled craftsmen supplemented by a specialist for the application of strain gauges and extensometers who worked part time on the job.

7 EXECUTION OF LOADING TEST

Three loading cycles were carried out. The first cycle with a maximum total load of 200 kN demonstrated that the concrete beam settled uniformly, which meant that the soil had been compacted uniformly, and that all measuring and loading devices functioned properly. In the second cycle, the model was loaded up to 800 kN and essentially a linear response was observed (fig. 4). In the third loading cycle the system was brought to failure at a maximum load of 1450 kN.

As the load versus settlement curve (fig. 4) shows, the model was loaded incrementally. In each case, the next increment of load was applied only when the time-dependent settlement-increase of the previous step had become negligible, which took about 40 minutes.

The total settlement of the concrete beam reached 2.9 mm under a contact pressure of 74 kN/m² in the first loading cycle. The rebound upon unloading was 0.7 mm. In the second cycle the reinforced soil was loaded up to 800 kN about 60 % of the predicted failure load which amounted to 1350 kN. The maximum settlement in the second cycle was 16.0 mm under 296 kN/m², and the rebound 2.7 mm.

During the third loading cycle, linear response of the model was observed up to about 1000 kN. Beyond this load, the load-settlement-curve became nonlinear and deformations of the reinforced soil body could be detected by eye. At about 1300 kN load which corresponds to an average contact pressure of 481 kN/m², the system started to yield and the next load increment to 1450 kN induced complete failure. At this stage the beam continued to settle under constant load. At a total vertical displacement of 121 mm which was reached after 1.5 hours the test was stopped because the maximum possible extension of the hydraulic jack of the loading device had been reached.

During the phase of plastic yielding of the retaining structure, a shallow but very well developed depression formed at the surface of the sand body. In front of it, the surface of the sand was bulging upwards. Behind the concrete beam there was a narrow depression, followed by a zone of upwards deformation. The topography of the upper surface of the model is presented on fig. 5. The fact that all features of the deformed shape are running parallel

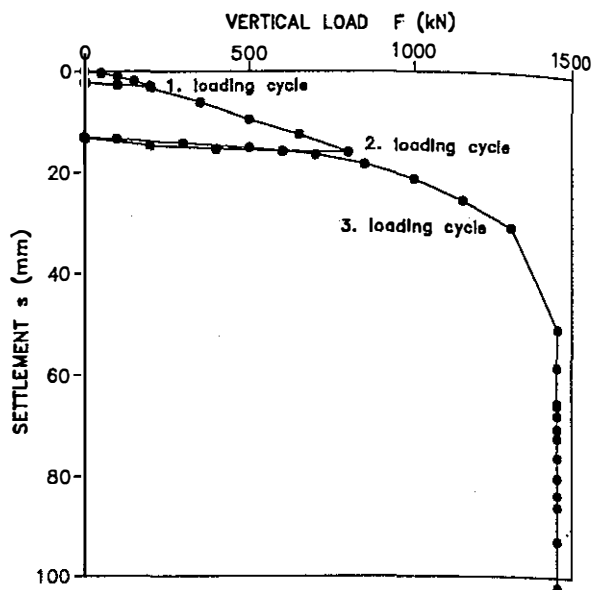


Fig.4 Load-settlement curve

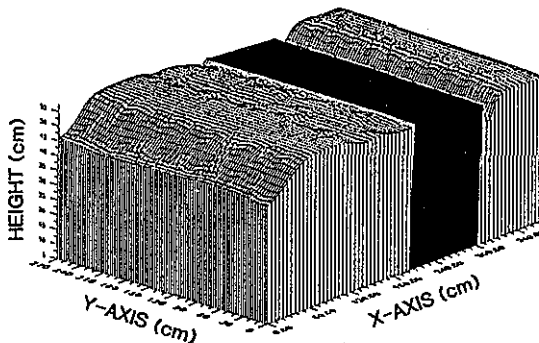


Fig.5 Topography of the upper surface after failure

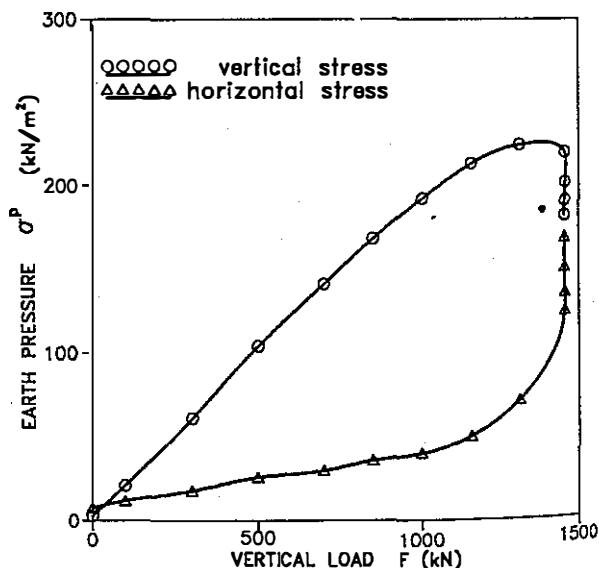


Fig.6 Maximum vertical and horizontal stress in the 5. layer

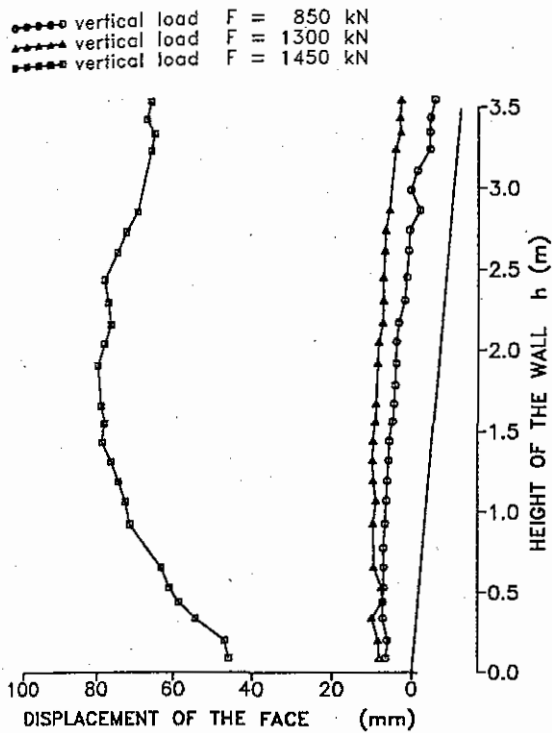


Fig.7 Horizontal deformation of the wall facing

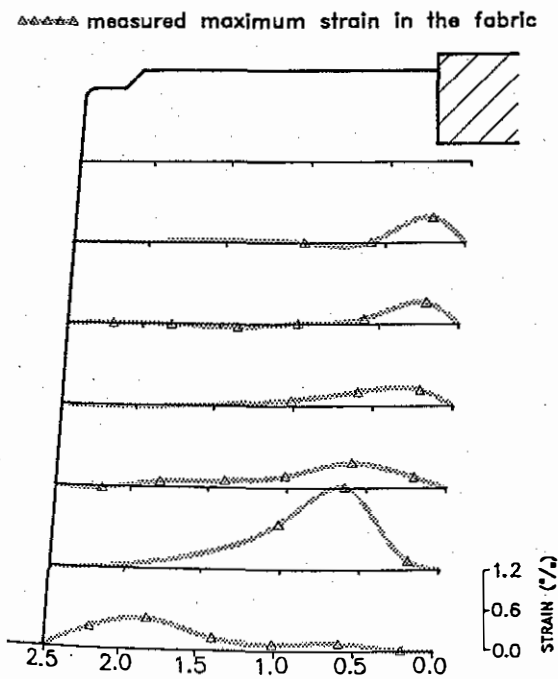


Fig.8 Distribution of maximum strains in each instrumented layer

to the face of the retaining structure supports the assumption of plane strain conditions. Evidently, the geosynthetic sandwiches at the side walls had performed efficiently in reducing wall friction to almost zero.

8 RESULTS

Since the stresses within the multilayered reinforced soil retaining structure without surcharge load were very low, measurements were taken only during the stage of vertical loading. The vertical stress components increased linearly with increasing external load until about $F = 1000$ kN as shown for example for the pressure cell in the 5. layer on fig. 6. The corresponding horizontal stress component is also increasing linearly until $F = 1000$ kN. It shows a pronounced progressive increase beyond this external load, indicating the transition from elastic to plastic behaviour, finally reaching the limit state condition.

The stress plot on fig. 6 is somewhat representative of the behaviour of the entire retaining structure. Below the loaded concrete beam, a stress distribution of the Boussinesq type develops and the soil body shows essentially linearly elastic behaviour until the structure yields. The lateral yield-displacement of the retaining structure causes the transition from at rest to active horizontal earth pressures under surcharge load as described by Coulomb's formula, this means the horizontal thrust almost doubles. At the same time a redistribution of the vertical stress components takes place.

The measurements of deformations and strains indicated a maximum displacement of the face of the reinforced earth body of up to 20 mm under a vertical load of 1300 kN which is less than 0.6 % of the height. At yielding conditions under the maximum possible load of 1450 kN, the lateral displacements reached about 80 mm which corresponds to about 2.3 % of the height of the retaining structure (fig. 7).

From observations of the earth pressure redistribution at failure and from strain- and displacement measurements (fig. 8), the failure surface sketched on fig. 9 could be deduced. It agrees very well with the assumptions made for the limit state analysis based on the kinematic element method.

As one might expect, the geogrid reinforcements experience only very small strains during at rest horizontal earth pressure conditions. Fig. 10 shows for example the strains measured at the far end of reinforcement layer 5. The strain increases almost linearly with the external load, and even under yield-load only a very slight nonlinearity can be observed. By contrast, the maximum strain in reinforcement layer 2 which is lower under at rest conditions than in layer 5 shows a sharp increase during yielding of the structure because it is located near the failure zone. But even though, the measured maximum strain of 1.2 % activates only a tensile force of 10 kN/m in the reinforcement which corresponds to 15 % of the short term tensile strength being very far from reinforcement breakage.

The model test leads to the conclusion, that the backfill soil is the weakest element of the tested composite structure under the pertinent conditions. Furthermore, the observed failure mode and yield-load are in good agreement with those predicted by the limit state equilibrium analysis based on the kinematic element method.

REFERENCES

Bundesminister für Verkehr, Abteilung Straßenbau.

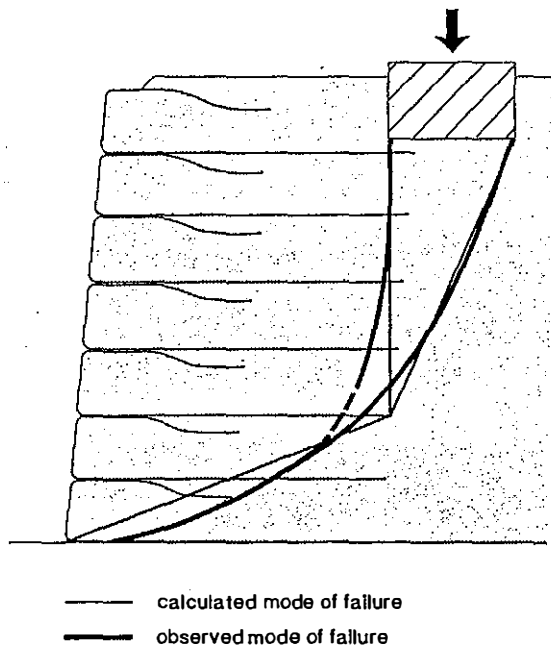


Fig.9 Comparison of the failure modes

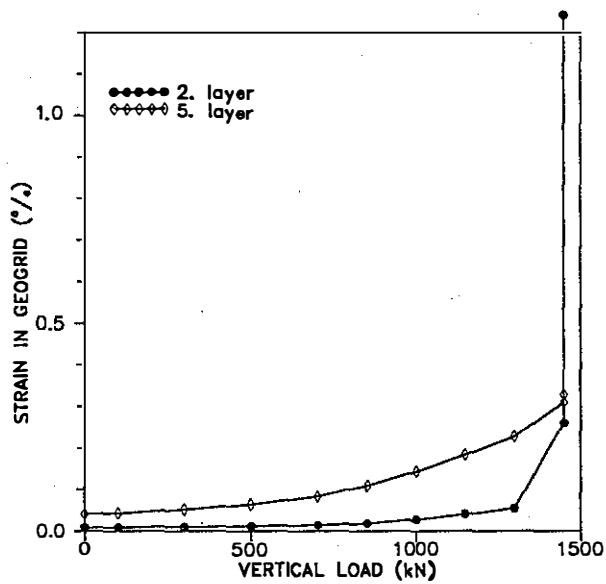


Fig.10 Strain measurements at selected points

Bedingungen für die Anwendung des Bauverfahrens
 Bewehrte Erde, 1985.

Pressl, G. & Zanzinger, H. 1991. *Benutzer-Handbuch, Programm: POWA*. LGA-Grundbauinstitut, Editor: Rehau AG + Co.

Schlösser, F. 1990. Mechanically Stabilized Earth Retaining Structures in Europe. *ASCE Geotechnical Special Publication No. 25*: 347 - 378.

Zanzinger, H. & Gartung E. 1992. Großmaßstäblicher Modellversuch einer Polsterwand aus Gittergewebe und Sand. *Veröffentlichungen des LGA-Grundbauinstitutes, Heft 62*.